

# Synthesis, crystal structure and hydrogenation properties of the ternary compounds $\text{LaNi}_4\text{Mg}$ and $\text{NdNi}_4\text{Mg}$

L. Guénée, V. Favre-Nicolin<sup>1</sup>, K. Yvon\*

Laboratoire de Cristallographie, Université de Genève, 24 quai E. Ansermet, CH-1211 Genève 4, Switzerland

Received 6 May 2002; accepted 17 May 2002

## Abstract

The title compounds have been prepared by induction melting and investigated with respect to structure and hydrogenation properties. Both crystallise with the cubic  $\text{MgCu}_4\text{Sn}$  type structure (space group  $F\bar{4}3m$ ,  $\text{LaNi}_4\text{Mg}$ :  $a = 7.17\text{--}7.18$  Å,  $\text{NdNi}_4\text{Mg}$ :  $a = 7.09875(1)$  Å) and absorb reversibly up to 4 hydrogen atoms per formula unit at 7–8 bar and  $\sim 50$  °C. Synchrotron and neutron powder diffraction data on deuterated  $\text{NdNi}_4\text{Mg}$  indicate an orthorhombic lattice distortion ( $\text{NdNi}_4\text{MgD}_{3.6}$ , space group  $Pmn2_1$ ,  $a = 5.0767(2)$ ,  $b = 5.4743(2)$ ,  $c = 7.3792(3)$  Å,  $\Delta V/V = 14.6\%$ ) and three almost fully occupied deuterium sites of which two are coordinated by a trigonal metal bipyramid ( $[\text{A}_2\text{B}_3]$  apices:  $\text{A} = 2\text{Nd}$ , base:  $\text{B} = 2\text{Ni}, \text{Mg}$ ) and one is coordinated by a metal tetrahedron ( $[\text{AB}_3]$   $\text{A} = \text{Nd}$ ,  $\text{B} = 3\text{Ni}$ ). The hydride is stable at room temperature under 1 bar hydrogen pressure, but desorbs rapidly at 80 °C under vacuum. Under air it decomposes by catalytic water formation.

© 2002 Elsevier Science B.V. All rights reserved.

**Keywords:** Hydrogen absorbing materials; Metal hydrides; Gas–solid reactions; Crystal structure; Neutron diffraction

## 1. Introduction

The search for new hydrogen storage compounds based on the  $\text{CaCu}_5$  type structure has led us to examine ternary R–Ni–Mg systems (R=Rare earths). A recent study of structure stability maps suggests [1] that compositions close to  $\text{RNi}_4\text{Mg}$  are outside the stability range of the  $\text{CaCu}_5$  type structure and inside the range of the  $\text{MgCu}_4\text{Sn}$  type structure. The latter can be considered as ordered ternary derivative of the  $\text{AuBe}_3$  type structure (space group  $F\bar{4}3m$ ) [2] in which Mg occupies the Au site ( $4a$ : 0 0 0, etc.) and Sn one of the Be sites ( $4c$ : 1/4 1/4 1/4, etc.). Known representatives containing R and Ni include cerium based  $\text{CeNi}_4\text{Mg}$  [3] and yttrium based  $\text{MgYNi}_4$  [4]. While the former compound was not investigated with respect to hydrogen absorption, the latter was found to absorb 3.6 hydrogen atoms per formula unit (H/f.u.) at ambient temperature and 30 bars hydrogen pressure [4]. The structure of the resulting hydride, however, was not

determined. On the other hand, lanthanum based compounds of composition  $\text{La}_{1-x}\text{Mg}_x\text{Ni}_2$  have been reported to crystallise with a disordered cubic  $\text{MgCu}_2$  (C15) type structure at low Mg contents ( $0 < x < 0.67$  [5]) and with the  $\text{MgNi}_2$  (C36) type structure at higher Mg contents ( $x > 0.67$ ). The composition  $(\text{La}_{0.5}\text{Mg}_{0.5})\text{Ni}_2 = \text{LaMgNi}_4$  was found to absorb up to 3.4 hydrogen atoms per formula unit [5]. In view of these results we decided to investigate  $\text{LaNi}_4\text{Mg}$  and its neodymium analogue  $\text{NdNi}_4\text{Mg}$  in more detail.

## 2. Experimental

### 2.1. Synthesis

The lanthanum compound was prepared by pressing La rods (Johnson Matthey, 99.99%) and Mg (Strem Chemicals, 99.8%) and Ni powders (Johnson Matthey, 5N) at the nominal composition  $\text{LaMg}_{1.108}\text{Ni}_{4.06}$  into pellets that were placed into a silver crucible and melted in an induction furnace under argon (6N). The as-cast alloys generally contained three phases ( $\text{MgNi}_2$ ,  $\text{LaNi}_2$  and elemental Ni) that were not well crystallised. In order to increase sample homogeneity and minimise evaporation

\*Corresponding author. Tel.: +41-22-702-6231; fax: +41-22-702-6864.

E-mail address: klaus.yvon@cryst.unige.ch (K. Yvon).

<sup>1</sup>Present address: European Synchrotron Radiation Facility ESRF, BP 220, F-38043 Grenoble Cedex, France.

losses magnesium was first pre-reacted with nickel to the binary metal compound  $\text{Mg}_2\text{Ni}$ , and pellets of powder mixtures of La,  $\text{Mg}_2\text{Ni}$  and Ni were then melted at various nominal compositions. The resulting weight losses did not exceed 2%. As-cast samples of nominal composition  $\text{La}_{1.08}\text{MgNi}_4$  consisted of a majority phase whose cubic cell parameter ( $a = 7.17 \text{ \AA}$ ) was within the previously reported range for the C15 type solid solution  $\text{La}_{1-x}\text{Mg}_x\text{Ni}_2$ . However, the presence of 200, 420, 600 and 640 diffraction planes in the X-ray patterns were not consistent with this structure type (space group  $Fd\bar{3}m$ ,  $h00: h = 4n$  and  $hk0: h + k = 4n$ ) and rather indicated a  $\text{MgCu}_4\text{Sn}$  type structure (space group  $F\bar{4}3m$ ). Furthermore, the samples contained two minority phases, one having the hexagonal  $\text{La}_2\text{Ni}_7$  type structure ( $a = 5.038$   $c = 24.35 \text{ \AA}$ ) and an unidentified phase that could be indexed on an orthorhombic C-centred lattice with cell parameters  $a = 4.21$ ,  $b = 10.27$  and  $c = 8.34 \text{ \AA}$ . In order to detect a possible deviation of the majority phase from the ideal metal ratio  $\text{Ni}/\text{Mg} = 4$  samples of composition  $\text{LaNi}_3\text{Mg}_2$  ( $\text{Ni}/\text{Mg} < 4$ ) and  $\text{LaNi}_{4.5}\text{Mg}_{0.5}$  ( $\text{Ni}/\text{Mg} > 4$ ) were prepared. The former was found to consist mainly of the cubic  $\text{LaNi}_4\text{Mg}$  phase and showed diffraction line broadening and splitting. The concentration of the non-identified orthorhombic phase was higher than in the  $\text{La}_{1.08}\text{MgNi}_4$  sample. The  $\text{LaNi}_{4.5}\text{Mg}_{0.5}$  sample contained  $\text{LaNi}_4\text{Mg}$ ,  $\text{LaNi}_5$  ( $\text{CaCu}_5$  type structure) and elemental Ni. None of the lanthanum alloys were annealed. For the neodymium compound compressed powder mixtures of Nd (Riedel–de Haën, >99.9%),  $\text{Mg}_2\text{Ni}$  and Ni of various nominal compositions were melted in an induction furnace and annealed for up to 33 h at 780–800 °C in quartz tubes filled by 0.3 bar argon (6N). The weight losses did not exceed 3%. All samples contained a majority phase having the  $\text{MgCu}_4\text{Sn}$  type structure and a minority phase (up to 25%) of binary  $\text{NdNi}_3$  having the  $\text{PuNi}_3$  type structure [6]. Samples of nominal composition  $\text{NdNi}_4\text{Mg}$  (#1),  $\text{Nd}_{1.008}\text{Ni}_4\text{Mg}$  (#2) and  $\text{Nd}_{1.038}\text{Ni}_4\text{Mg}_{1.087}$  (#3) were used for hydrogen absorption, synchrotron diffraction and pressure-composition–isotherm/neutron diffraction measurements, respectively.

## 2.2. Structure analysis of alloys

The alloy samples  $\text{LaNi}_3\text{Mg}_2$  and  $\text{NdNi}_4\text{Mg}$  (#2) were investigated by synchrotron powder diffraction (ESRF, Grenoble, SNBL, capillaries of 0.3 mm diameter). For the lanthanum sample, the pattern ( $\lambda = 0.85022 \text{ \AA}$ ) confirmed the presence of two phases, one having the  $\text{MgCu}_4\text{Sn}$  type structure and thus the likely composition  $\text{LaNi}_4\text{Mg}$  (La, Ni and Mg on Mg, Cu and Sn sites, respectively), and the other a hitherto unknown orthorhombic C-centred structure. The diffraction lines of the  $\text{LaNi}_4\text{Mg}$  phase were split and had to be modelled during structure refinement by the assumption of two  $\text{MgCu}_4\text{Sn}$  type phases having the cell

parameters  $a = 7.18$  and  $7.17 \text{ \AA}$ . However, the quality of the data was insufficient to derive reliable Mg/Ni ratios for either one of the phases and thus prove their different chemical compositions. For the neodymium sample, synchrotron data were collected at  $\lambda = 0.50012 \text{ \AA}$  within the angular range  $2\theta = 3.02^\circ$ – $33.26^\circ$  in steps of  $0.004^\circ$ . The sample contained two phases of which the principal one could be attributed to a  $\text{NdNi}_4\text{Mg}$  phase crystallising with the  $\text{MgCu}_4\text{Sn}$  type structure and the minor one to a  $\text{NdNi}_3$  phase crystallising with the  $\text{PuNi}_3$  type structure. The structures were refined by using the program Fullprof [7] and by varying 21 parameters ( $\text{NdNi}_4\text{Mg}$ : 6 structural + 5 profile + scale factor;  $\text{PuNi}_3$ : 9 structural, 1 scale). For  $\text{NdNi}_4\text{Mg}$  a small substitution of Ni by Mg (site 4c) allowed to improve the agreement indices, in particular  $R_{\text{Bragg}}$ . The patterns are represented in Fig. 1 and refinement results are summarised in Table 1.

## 2.3. Hydrogen absorption and desorption

Due to the relatively large concentration of secondary phases in the lanthanum samples the hydrogen absorption properties were mainly studied on the neodymium samples. One of the latter (#1, nominal composition  $\text{NdNi}_4\text{Mg}$  annealed at 800 °C for 24 h) was powdered in a glove box and introduced into a microbalance (Hiden Analytical) that was evacuated for a few hours under preliminary vacuum ( $10^{-3}$  bar). Hydrogenation was carried out under a pressure of 7 bars at 50 °C for 24 h. After a few minutes the sample started to absorb slowly but steadily as shown in Fig. 2. After about 3 h the weight increase levelled off at a value corresponding to about 3.6 H/f.u. (value corrected for the presence of ~26 wt.% hydrogen inert  $\text{NdNi}_3$  phase, see ch. 2.4). A pressure–composition–isotherm ( $p$ – $c$ – $T$ ) obtained under the same conditions on part of another sample (#3, nominal composition  $\text{Nd}_{1.038}\text{Mg}_{1.087}\text{Ni}_4$ , annealed at 780 °C for 28 h, 18% secondary  $\text{NdNi}_3$  phase) is shown in Fig. 3. The  $\text{NdNi}_4\text{Mg}$  phase absorbs up to 4 H/f.u. (value corrected for the presence of hydrogen inert  $\text{NdNi}_3$  phase). One notices a relatively narrow (~2 H/f.u.) and ill-defined plateau region at  $p(\text{H}_2) \sim 1$  bar, followed by a relatively wide (2H/u.f.) single-phase domain at higher pressures. Thus the hydrogenation properties of  $\text{NdNi}_4\text{Mg}$  are rather different from those of  $\text{LaNi}_5$  type hydrides for which long plateaus and narrow single phase domains were found [8]. The absorption/desorption kinetics is relatively slow, thus precluding  $p$ – $c$ – $T$  measurements. After the experiment, the sample was investigated by X-ray diffraction in air, and then replaced into the thermobalance and evacuated at 80 °C for a few hours. The patterns indicated almost complete loss of hydrogen and recovery of the initial alloy structure. Interestingly, after the hydrogenated samples were exposed to air in a glass container, water droplets appeared after a few hours on the surface of the container walls. No such effects occurred if the hydride was kept in the glove box. Finally, one sample (#2,

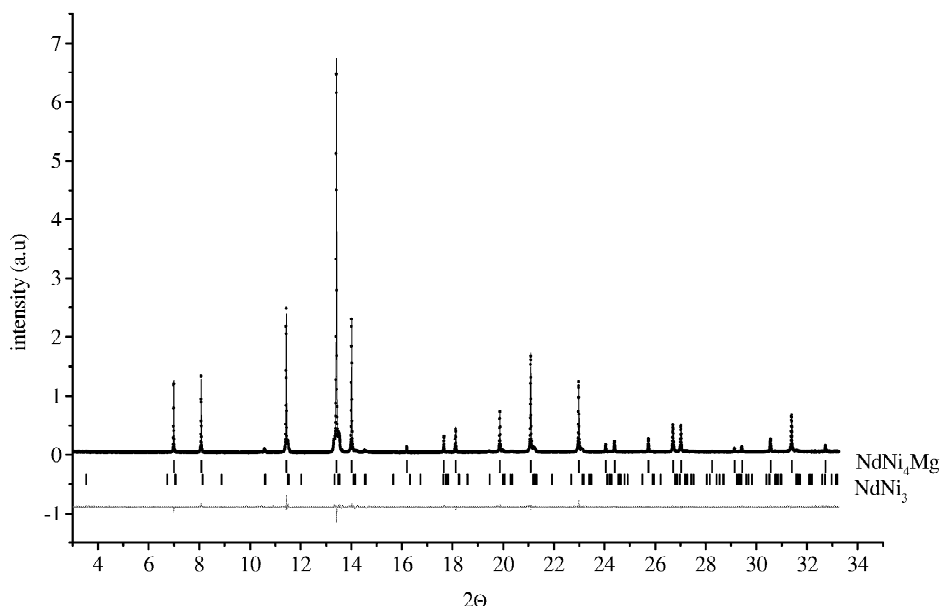


Fig. 1. Observed (points), calculated (line) and difference (bottom line) synchrotron powder diffraction pattern of NdNi<sub>4</sub>Mg (sample #2,  $\lambda = 0.50012$  Å). Vertical bars indicate Bragg position of contributing phases NdNi<sub>4</sub>Mg (74%, top) and NdNi<sub>3</sub> (26%, bottom).

nominal composition Nd<sub>1.008</sub>Ni<sub>4</sub>Mg, 25% secondary NdNi<sub>3</sub> phase) was hydrogenated in an autoclave at 7 bar and 50 °C during a few hours for the synchrotron diffraction study, and part of another sample (#3) was deuterated under 7.5 bars at 50 °C for the neutron diffraction study. As for the lanthanum compound, hydrogenation experiments were performed on a sample of nominal composition La<sub>1.08</sub>Ni<sub>4</sub>Mg. The multiphase sample (containing the secondary phases La<sub>2</sub>Ni<sub>7</sub> and the non-identified orthorhombic C-centred phase) was placed into the microbalance and exposed to hydrogen of 8 bars pressure at 53 °C. The observed weight increase was found to correspond to a hydrogen uptake of ~5 H/f.u. However, in view of the

presence of hydrogen absorbing secondary phases this value is presumably lower (see Section 2.4).

#### 2.4. Structure analysis of hydrides (deuterides)

Preliminary Guinier X-ray diagrams of the hydrogenated neodymium samples revealed significant structural changes of the metal atom substructure. One sample (#2) was re-measured by synchrotron radiation (ESRF, SNBL,  $\lambda = 0.50012$  Å, capillary  $\varnothing$  0.3 mm). Although it partially desorbed during the measurement the pattern of the main hydride phase could be indexed on an orthorhombic lattice having the cell parameters  $a = 5.0788(2)$ ,  $b = 5.4887(2)$ ,  $c = 7.3846(2)$  Å. The cell parameter relationships with the hydrogen free cubic compound are  $a_{\text{ortho}} \approx a_{\text{cub}}/\sqrt{2}$ ,  $b_{\text{ortho}} \approx a_{\text{cub}}/\sqrt{2}$ ,  $c_{\text{ortho}} \approx a_{\text{cub}}$ ;  $V_{\text{ortho}} = 1/2 V_{\text{cub}}$ , and the relative volume increase during hydrogenation is  $\Delta V/V = 15.1\%$ . The systematically absent reflections suggested non-centrosymmetric space group  $Pmn2_1$ . Centrosymmetric  $Pmnm$  was rejected because it precludes a continuous (non-reconstructive) transition from intermetallic NdNi<sub>4</sub>Mg to the hydride. The metal atom substructure was solved ab initio by the newly developed computer program FOX [9]. However, due to the partial desorption of the sample during the measurement a satisfactory structure refinement on these data was not possible. Neutron diffraction data on a deuterated sample (#3) were collected on the powder diffractometer HRPT at SINQ (PSI, Villigen, high resolution mode,  $\lambda = 1.494$  Å, scattering range  $2.95 < 2\theta < 162.90^\circ$ , step size  $\Delta 2\theta = 0.05^\circ$ , vanadium container). The deuterium substructure was determined by FOX by introducing 7 deuterium atoms per unit cell at

Table 1

Structure refinement results on synchrotron powder diffraction data for NdNi<sub>4</sub>Mg

Phase 1: NdNi <sub>4</sub> Mg (MgCu <sub>4</sub> Sn type structure, refined content ~74 wt.%)						
space group, $F\bar{4}3m$ , $a = 7.09875(1)$ Å						
Atoms	Site	$x$	$y$	$z$	$B$ (Å <sup>2</sup> )	Occupancy
Nd	4a	0	0	0	0.34(2)	1.0
Mg	4c	1/4	1/4	1/4	0.5(1)	0.912(7)
Ni1	4c	1/4	1/4	1/4	$B_{\text{Mg}}$	1–Mg
Ni2	16e	0.62376(6)	$x$	$x$	0.50(2)	1.0

$$R_{\text{Bragg}} = 1.92\%, N_{\text{ref}}^a = 26, 12 \text{ variables}$$

Phase 2: NdNi<sub>3</sub> (PuNi<sub>3</sub> type structure, refined content ~26 wt.%)  
space group  $R\bar{3}m$ ,  $a = 4.9918(2)$ ,  $c = 24.334(1)$  Å

$$R_{\text{Bragg}} = 12.1\%, N_{\text{ref}}^a = 133, 10 \text{ variables}$$

$$R_{\text{p}} = 13.7\%, R_{\text{wp}} = 12.8\%, \text{Chi}^2 = 3.11$$

Sample #2, two phases, e.s.d.'s in parentheses.

<sup>a</sup>  $N_{\text{ref}}$ : number of observed reflections.

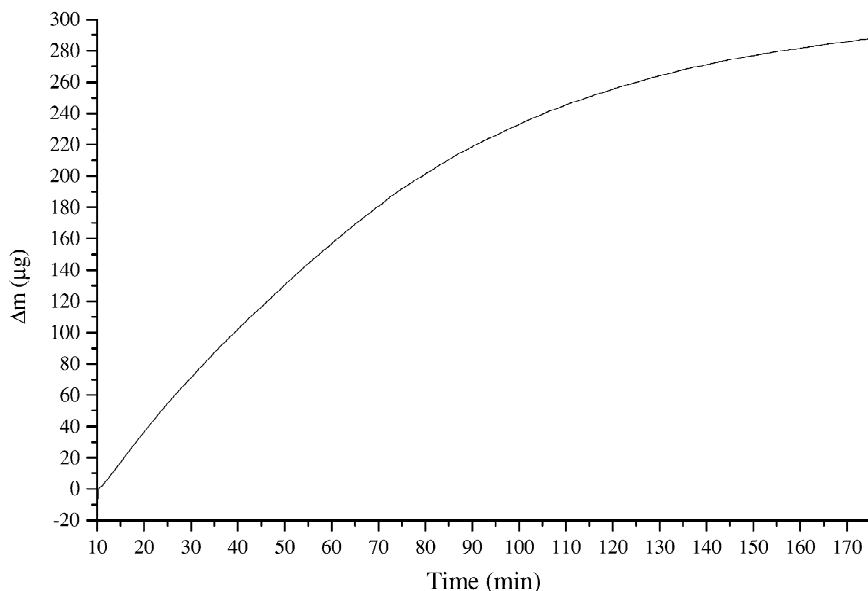


Fig. 2. Mass increase ( $\mu\text{g}$ ) versus hydrogen uptake (H/f.u.) of  $\text{NdNi}_4\text{Mg}$  sample #1 in microbalance ( $T=50^\circ\text{C}$ , 7 bars hydrogen pressure, initial sample weight 42.55 mg, total weight variation  $\Delta m = 287.6 \mu\text{g}$ , maximum hydrogen content 3.6 H/f.u., values corrected for the presence of 25 wt.% hydrogen inert  $\text{NdNi}_3$  phase).

random positions and fixing the metal atom substructure in space group  $Pmn2_1$ . Three independent D sites with practically full occupancy were found at sites  $4b$  ( $x, y, z$  etc.) and  $2a$  ( $0, y, z$  etc.). Structure refinement of the two-phase sample was performed by Fullprof [7] by varying a total of 46 parameters of which 28 were atomic parameters of the  $\text{NdNi}_4\text{MgD}_{3.6}$  phase. No deuterium sites were identified in the secondary  $\text{NdNi}_3$  phase as expected from its cell parameters that remained practically un-

changed after deuteration. Results are summarised in Table 2, and the diffraction patterns are represented in Fig. 4. As to the hydrogenated lanthanum samples, Guinier X-ray diagrams revealed an orthorhombic lattice distortion of the  $\text{LaNi}_4\text{MgH}_x$  phase (estimated cell parameters  $a=5.12$ ,  $b=5.54$ ,  $c=7.47 \text{ \AA}$ ; relative volume expansion  $\Delta V/V \sim 15\%$ ) similar to that of the neodymium analogue, thus suggesting similar amounts of absorbed hydrogen ( $\sim 3.6$  H/u.f).

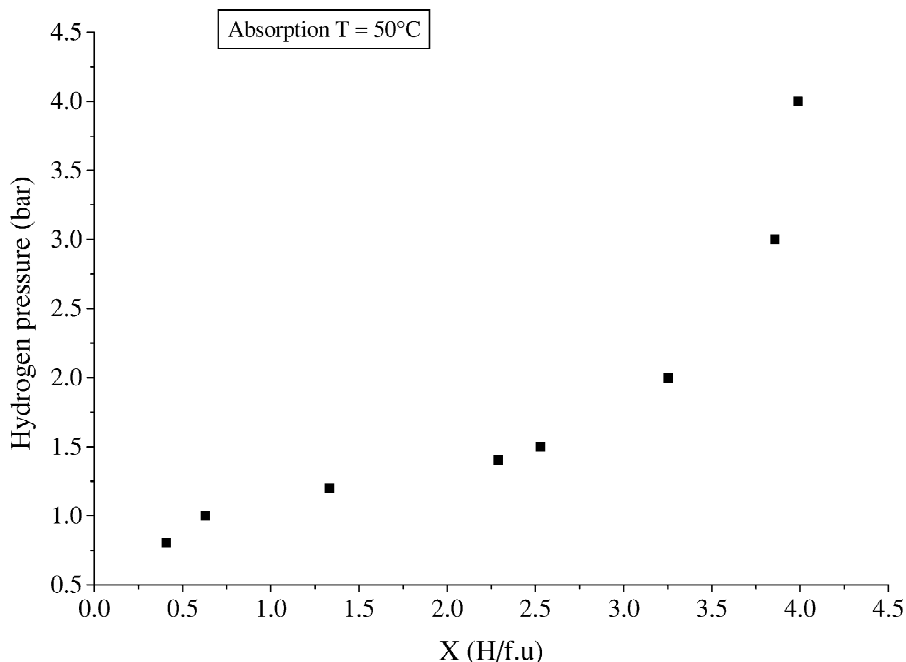


Fig. 3. Pressure–composition isotherm of  $\text{NdNi}_4\text{Mg}$  sample #3 ( $T=50^\circ\text{C}$ , composition corrected for 18 wt.% hydrogen inert  $\text{NdNi}_3$  phase; maximum hydrogen content 4 H/f.u.).

Table 2

Structure refinement results on neutron powder diffraction data for the deuteride NdNi<sub>4</sub>MgD<sub>3.6</sub>Phase 1: NdNi<sub>4</sub>MgD<sub>3.6</sub> (refined content ~83 wt.%)space group *Pmn*2<sub>1</sub>, *a* = 5.0767(2), *b* = 5.4743(2), *c* = 7.3792(3) Å, Δ*V*/*V*<sup>a</sup> = 14.6%

Atoms	Site	<i>x</i>	<i>y</i>	<i>z</i>	<i>B</i> (Å <sup>2</sup> )	Occupancy
Nd	2 <i>a</i>	0	0.302(1)	0.0	0.91(9)	1.0
Mg	2 <i>a</i>	0	0.813(2)	0.223(1)	2.3 (2)	1.0
Ni1	2 <i>a</i>	0	0.4519(7)	0.6233(8)	0.68(5)	1.0
Ni2	2 <i>a</i>	0	0.9935(7)	0.6053(8)	0.65(5)	1.0
Ni3	4 <i>b</i>	0.7505(7)	0.2270(4)	0.3811(6)	0.42(3)	1.0
D1	4 <i>b</i>	0.7462(7)	0.5089(7)	0.7544(9)	1.26(7)	0.921(9)
D2	2 <i>a</i>	0	0.716(1)	0.513(1)	2.1(1)	0.891(1)
D3	2 <i>a</i>	0	0.9458(9)	0.8245(9)	0.4(1)	0.899(1)

*R*<sub>Bragg</sub> = 3.8%, *N*<sub>ref</sub> = 296, 32 variablesPhase 2: NdNi<sub>3</sub>, (PuNi<sub>3</sub> type structure, refined content ~17 wt.%)space group *R*3̄*m*, *a* = 4.995(2), *c* = 24.19(1) Å*R*<sub>Bragg</sub> = 4.9%, *N*<sub>ref</sub><sup>b</sup> = 195, 14 variables*R*<sub>p</sub> = 8.3%, *R*<sub>wp</sub> = 9.0%, *Chi*<sup>2</sup> = 9.01

Sample #3, 2 phases, e.s.d.'s in parentheses.

<sup>a</sup> Relative volume increase during deuteration (*V*<sub>cub</sub> = 2*V*<sub>ortho</sub>).<sup>b</sup> *N*<sub>ref</sub>: number of observed reflections.

### 3. Discussion

#### 3.1. Structure of intermetallic compounds

The structure analysis confirms that both LaNi<sub>4</sub>Mg and NdNi<sub>4</sub>Mg crystallise with ordered MgCu<sub>4</sub>Sn type structures. Although they can be formally derived from the cubic AuBe<sub>5</sub> type structure, their crystal chemistry and structural analogy between Mg and La(Nd) sites suggest that they should rather be considered as derivatives of the cubic C15 type structure, in agreement with structure

stability maps [1]. Interestingly, the lanthanum compound lies within the compositional range of the La<sub>1-x</sub>Mg<sub>x</sub>Ni<sub>2</sub> series (0 < *x* < 0.67) for which a disordered C15 type structure has been reported, and its cell parameter (LaNi<sub>4</sub>Mg: 7.17–7.18 Å) is significantly larger than that of the C15 type structure having the same composition (La<sub>0.5</sub>Mg<sub>0.5</sub>Ni<sub>2</sub>: *a* = 7.149 Å [5]). This polymorphism may be attributed to different sample preparation conditions. Small deviations from RNi<sub>4</sub>Mg stoichiometry are possible in view of the range of cell parameters found for the lanthanum compound (7.17–7.18 Å) and the slight occupa-

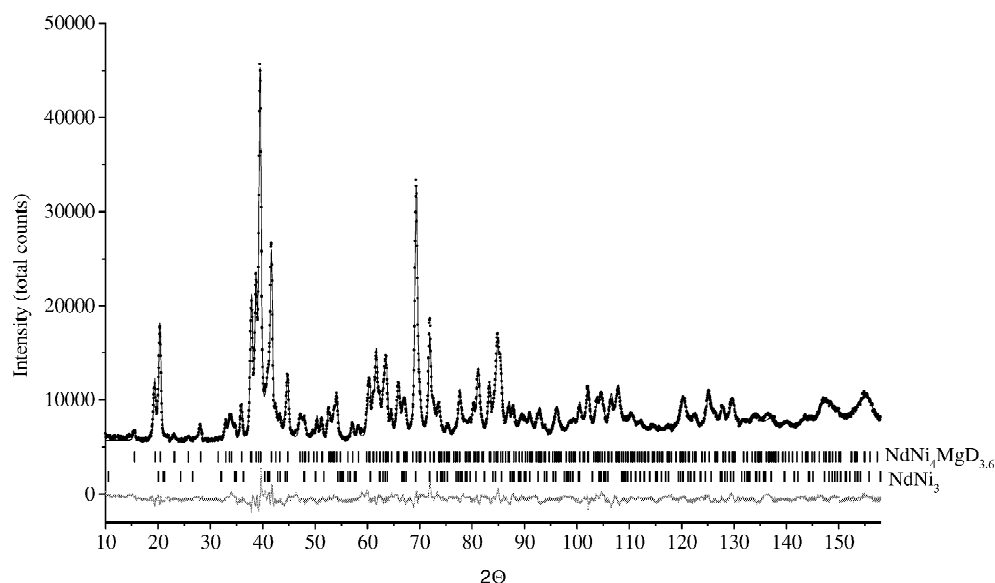


Fig. 4. Observed (points), calculated (line) and difference (bottom line) neutron diffraction pattern of NdNi<sub>4</sub>MgD<sub>3.6</sub> (sample #3, λ = 1.494 Å). Vertical bars indicate Bragg positions of contributing phases NdNi<sub>4</sub>MgD<sub>3.6</sub> (83%, top) and NdNi<sub>3</sub> (17%, bottom).

tional disorder found for the neodymium compound (site 4c is occupied 91% by magnesium and 9% by nickel). Given their relatively high atom coordination numbers

(CN=16 for R and Mg, CN=12 for Ni) the structures can be considered as topologically close packed. The interatomic distances (Table 3) are in the usual range.

Table 3  
Comparison between metal–metal distances in cubic NdNi<sub>4</sub>Mg and orthorhombic NdNi<sub>4</sub>MgD<sub>3.6</sub>

NdNi <sub>4</sub> Mg		<i>F</i> $\bar{4}$ 3 <i>m</i>		NdNi <sub>4</sub> MgD <sub>3.6</sub>		<i>Pmm</i> 2 <sub>1</sub>	
Central atom	CN <sup>a</sup>	Coordinated atoms	Distance <sup>b</sup> (Å)	Central atom	CN <sup>a</sup>	Coordinated atoms	Distance (Å)
Nd	16	12 Ni	2.9471(4)	Nd	16	1 Ni1	2.899 (6)
		4 Mg	3.0750(0)			2 Ni3	3.007 (5)
Mg	16	12 Ni	2.9418(4)	Mg	16	2 Ni1	3.015 (4)
		4 Nd	3.0750(0)			2 Ni2	3.108 (4)
Ni	12	3 Ni <sup>c</sup>	2.4860(6)	Ni1	12	2 Ni3	3.111 (4)
		3 Ni <sup>c</sup>	2.5360(6)			1 Mg	3.14 (1)
		3 Nd	2.9471(4)			1 Mg	3.25 (1)
		3 Mg	2.9418(4)			2 Ni3	3.281 (6)
Ni	12			Ni2	12	2 Mg	3.319 (6)
						1 Ni2	3.366 (6)
						2 Ni3	2.835 (9)
						2 Ni3	2.844 (5)
						2 Ni2	2.884 (5)
						1 Ni2	2.99 (1)
						2 Ni1	3.016 (6)
						1 Nd	3.14 (1)
						1 Nd	3.25 (1)
						2 Nd	3.319 (6)
						1 Ni1	3.55 (1)
						2 Ni3	3.64 (1)
				Ni3	12	2 Ni3 <sup>c</sup>	2.513 (6)
						1 Ni2 <sup>c</sup>	2.513 (5)
						2 Ni3 <sup>d</sup>	2.886 (6)
						1 Ni2 <sup>d</sup>	2.968 (5)
						1 Nd	2.899 (6)
						2 Nd	3.015 (4)
						2 Mg	3.016 (6)
						1 Mg	3.55 (1)
						2 Ni3 <sup>c</sup>	2.444 (6)
						1 Ni1 <sup>c</sup>	2.513 (5)
						2 Ni3 <sup>d</sup>	2.686 (6)
						1 Ni1 <sup>d</sup>	2.968 (5)
				2 Mg	2.884 (5)		
				1 Mg	2.99 (1)		
				2 Nd	3.108 (4)		
				1 Nd	3.366 (6)		
				1 Ni2 <sup>c</sup>	2.444 (6)		
				1 Ni1 <sup>c</sup>	2.513 (6)		
				1 Ni3 <sup>c</sup>	2.533 (5)		
				1 Ni3 <sup>d</sup>	2.543 (5)		
				1 Ni2 <sup>d</sup>	2.686 (6)		
				1 Ni1 <sup>d</sup>	2.886 (6)		
				1 Mg	2.844 (9)		
				1 Mg	2.835 (9)		
				1 Nd	3.007 (6)		
				1 Nd	3.111 (4)		
				1 Nd	3.281 (6)		
				1 Mg	3.64 (1)		

<sup>a</sup> CN: coordination number.

<sup>b</sup> Calculated with  $a = 7.10215(2)$  Å.

<sup>c</sup> Uncapped Ni<sub>4</sub> tetrahedra.

<sup>d</sup> Ni<sub>4</sub> tetrahedra capped by D atoms (see text).

### 3.2. Hydrogen absorption

NdNi<sub>4</sub>Mg and LaNi<sub>4</sub>Mg absorb about the same quantity of hydrogen (NdNi<sub>4</sub>Mg sample #1: 0.60 H/metal atom, sample #3: 0.67 H/metal atom) as isostructural YNi<sub>4</sub>Mg under similar conditions (0.6 H/metal atom [4]), but less than C15 type La<sub>0.5</sub>Mg<sub>0.5</sub>Ni<sub>2</sub> (1.1 H/metal atom at room temperature and  $P=10$  bars [5]). Similar to the latter, NdNi<sub>4</sub>Mg and LaNi<sub>4</sub>Mg have relatively slow kinetics and do not tend to decompose and/or become amorphous during hydrogenation. However, in contrast to La<sub>0.5</sub>Mg<sub>0.5</sub>Ni<sub>2</sub> that tends to segregate into LaH<sub>3</sub>, MgH<sub>2</sub> and Ni during desorption at 80 °C, no segregation was observed for NdNi<sub>4</sub>Mg during desorption at 80 °C under vacuum during a few hours. In fact, the compound released almost quantitatively its hydrogen and returned to the initial cubic MgCu<sub>4</sub>Sn-type structure without a significant change in cell parameter.

### 3.3. Structure of deuteride

The refined deuterium content of NdNi<sub>4</sub>MgD<sub>x</sub> ( $x = 3.63(2)$ ) is in good agreement with that determined for the hydride on the microbalance (sample #1:  $x = 3.6$ , #3:  $x = 4$ ). During deuteration the metal atom substructure undergoes important changes as shown by the symmetry reduction from cubic to orthorhombic, the strongly anisotropic lattice expansion ( $\Delta b/b = 9.3\%$ ,  $\Delta c/c = 4.0\%$ ,  $\Delta a/a = 1.2\%$ ) and the unequal lengthening of the Ni–Ni bonds (see below). The three deuterium sites are nearly fully occupied thus suggesting the upper phase limit to be near the composition NdNi<sub>4</sub>MgD<sub>4</sub>. The metal coordinations of the D sites are represented in Fig. 5 and the corresponding bond distances are summarised in Table 4. Two sites (D1, D2) are coordinated by trigonal metal bipyramids ([A<sub>2</sub>B<sub>3</sub>] apices: A = 2Nd, base: B = 2Ni, Mg) with bond distances D–Nd = 2.48–2.54 Å, D–Mg = 2.17, 2.21 Å, D–Ni = 1.64–1.72 Å, and one (D3) is coordinated by a metal tetrahedron ([AB<sub>3</sub>] A = Nd, B = 3Ni) with bond distances D–Nd = 2.34 (Nd) and D–Ni = 1.64 Å. The corresponding radii of the metal interstices ( $R_{\text{site}}$ ) as calculated within the hard sphere approximation are larger than 0.43 Å and thus consistent with Westlake's model [10]. Although the displacement amplitudes of the deuterium atoms in the trigonal bipyramids (D1, D2) are somewhat larger than those in the tetrahedra (D3), they suggest triangular ([MgNi<sub>2</sub>] type) rather than tetrahedral ([NdMgNi<sub>2</sub>] type) nearest neighbour environment within the bipyramids. An alternative way to rationalise the structure is to consider the deuterium atoms as bridging ligands of Ni<sub>4</sub> tetrahedra. As shown in Fig. 6, this corresponds to the presence of [Ni<sub>4</sub>D<sub>4</sub>] units in which one face (Ni<sub>3</sub>–Ni<sub>3</sub>–Ni<sub>2</sub>) and three edges (two Ni<sub>1</sub>–Ni<sub>3</sub>, one Ni<sub>1</sub>–Ni<sub>2</sub>) are capped by D3, D1 and D2 atoms, respectively. As expected, the capped Ni<sub>4</sub> tetrahedra (Ni–Ni = 2.54–2.97 Å) are considerably expanded

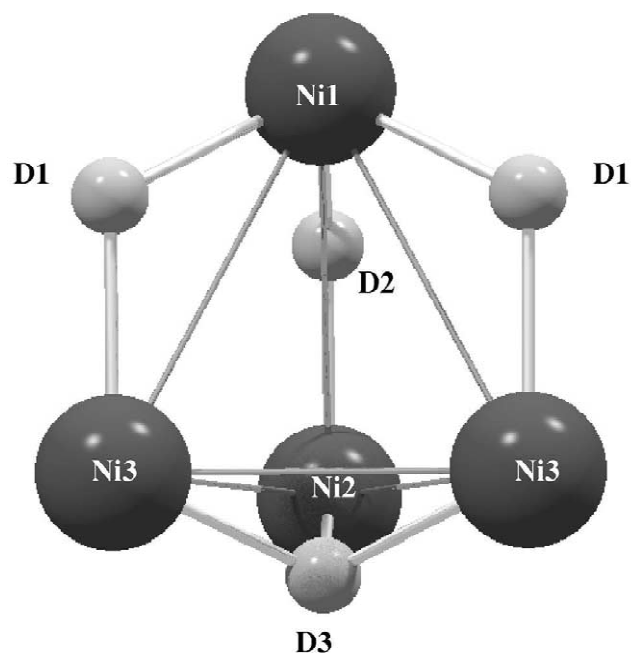


Fig. 5. Bridging deuterium ligands in [Ni<sub>4</sub>D<sub>4</sub>] unit, viewed approximately along the mirror plane (point group symmetry  $m$ ).

Table 4  
Metal–deuterium bond distances, D–D contact distances and interstitial hole size ( $R_{\text{site}}$ ) in NdNi<sub>4</sub>MgD<sub>3.6</sub>, e.s.d.'s in parentheses

Atom	Site	Coordinated atoms	Distance <sup>a</sup> (Å)	$R_{\text{site}}$ (Å) <sup>b</sup>
Nd	2a	1D3	2.340(7)	
		2D1	2.482(6)	
		2D1	2.496(6)	
		2D2	2.5422(6)	
Mg	2a	2D1	2.174(9)	
		1D2	2.21(1)	
Ni1	2a	2D1	1.641(6)	
		1D2	1.66(1)	
Ni2	2a	1D3	1.639(9)	
		1D2	1.66(1)	
Ni3	4b	1D3	1.639(5)	
		1D1	1.722(6)	
D1	4b	Nd	2.482(6)	0.47
		Nd	2.496(6)	
		Mg	2.174(9)	
		Ni3	1.722(6)	
		Ni1	1.641(6)	
D2	2a	2 Nd	2.5422(6)	0.47
		Mg	2.21(1)	
		Ni1	1.66(1)	
		Ni2	1.66(1)	
D3	2a	Nd	2.340(7)	0.43
		Ni2	1.639(9)	
		2 Ni3	1.639(5)	

<sup>a</sup> D–Ni cut-off distance <3.0 Å.

<sup>b</sup> Calculated from atomic radii  $R_{\text{Nd}} = 1.821$  Å,  $R_{\text{Mg}} = 1.602$  Å,  $R_{\text{Ni}} = 1.246$  Å [11].

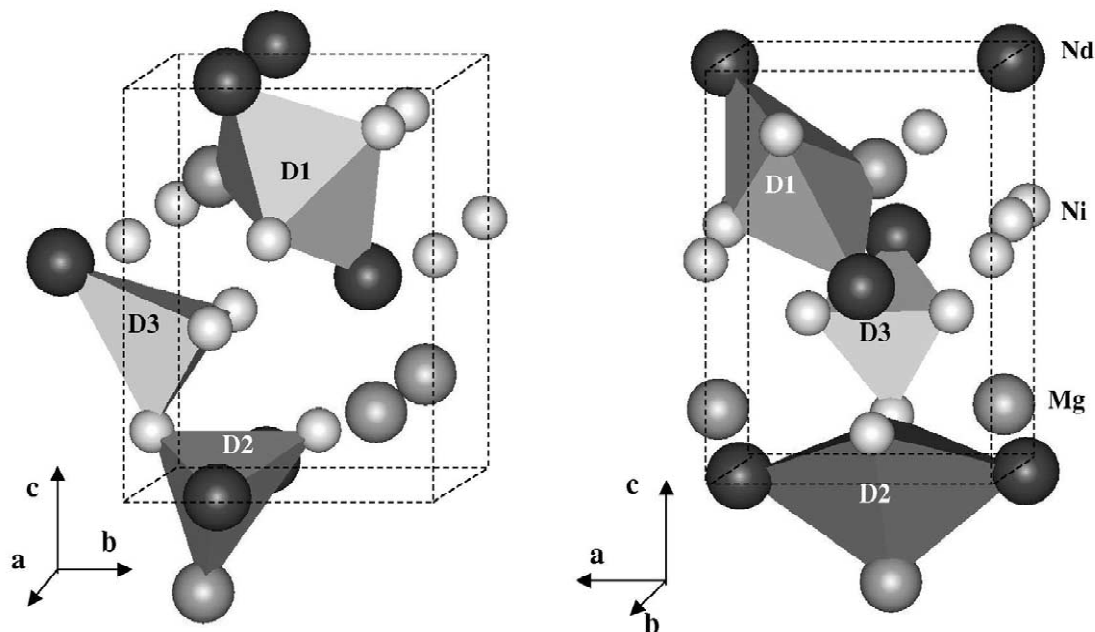


Fig. 6. Metal coordinations of deuterium sites in orthorhombic  $\text{NdNi}_4\text{MgD}_{3.6}$  viewed along two perpendicular directions. For clarity, only one representative of each site is drawn.

(by up to  $0.5 \text{ \AA}$ ) compared to the uncapped ones ( $\text{Ni-Ni} = 2.44\text{--}2.51 \text{ \AA}$ , see Table 3) that have about the same size as those in the deuterium free cubic compound  $\text{NdNi}_4\text{Mg}$  ( $\text{Ni-Ni} = 2.49\text{--}2.54 \text{ \AA}$ ). The D–D distances are all longer than  $2.5 \text{ \AA}$  and thus indicative for repulsive D–D interactions.

#### 4. Conclusions

$\text{LaNi}_4\text{Mg}$  and  $\text{NdNi}_4\text{Mg}$  absorb reversibly up to 4 hydrogen atoms per formula unit at 7 bars and  $50^\circ\text{C}$  without amorphisation or segregation into binary hydrides. Although their hydrogen density ( $\text{NdNi}_4\text{MgH}_4$ : 0.99 wt.%,  $65.05 \text{ g H}_2 \text{ l}^{-1}$ ) and absorption/desorption kinetics are somewhat lower than that of  $\text{CaCu}_5$  type hydrides, their  $p$ – $c$ – $T$  isotherms are in a useful range for hydrogen storage applications. Hydrogenation leads to an orthorhombic distortion of the cubic  $\text{MgCu}_4\text{Sn}$  type metal host structure in which hydrogen occupies one tetrahedral  $[\text{AB}_3]$  ( $\text{A}=\text{Nd}$ ,  $\text{B}=3\text{Ni}$ ) and two triangular bipyramidal coordinated  $[\text{A}_2\text{B}_3]$  metal sites ( $\text{A}=2\text{Nd}$ , base:  $\text{B}=2\text{Ni}, \text{Mg}$ ) in a nearly ordered configuration. In cubic C15 type hydrides of similar composition, hydrogen is disordered exclusively over tetrahedral sites of type  $[\text{A}_2\text{B}_2]$ . Finally,  $\text{NdNi}_4\text{MgH}_x$  and presumably also  $\text{LaNi}_4\text{MgH}_x$  desorb hydrogen rapidly in air by catalytic water formation. A similar phenomenon was already observed for the

C15 type  $\text{La}_{1-x}\text{Mg}_x\text{Ni}_2$  hydrides but its mechanism is unknown.

#### Acknowledgements

The authors thank D. Sheptyakov (PSI, Villigen) for help with collecting the neutron diffraction data on HRPT at SINQ, and the staff of the Swiss Norwegian beamline at ESRF (Grenoble) for help with collecting the synchrotron data. Thanks are also due to R. Cerny (Geneva) for useful discussions. This work was supported by the Swiss National Science Foundation and the Swiss Federal Office of Energy.

#### References

- [1] L. Guénée, PhD thesis No. 3341, University of Geneva (2002).
- [2] K. Osamura, Y. Murakami, *J. Less-Common Met.* 60 (1978) 311–313.
- [3] C. Geibel, U. Klinger, M. Weiden, B. Buschinger, F. Steglich, *Physica B* 237–238 (1997) 202–204.
- [4] K. Aono, S. Orimo, H. Fujii, *J. Alloys Comp.* 309 (2000) L1–L4.
- [5] H. Oesterreicher, H. Bittner, *J. Less-Common Met.* 73 (1980) 339–344.
- [6] A.V. Virkar, A. Raman, *J. Less-Common Met.* 18 (1969) 59–66.
- [7] J. Rodríguez-Carvajal, in: Abstract of the Satellite Meeting on Powder Diffraction, Congress of the International Union of Crystallography, Toulouse, France, 1990, p. 127; Fullprof Program, version 3.5d Oct 98-LLB-JRC, 1998.

- [8] C. Lartigue, A. Percheron-Guégan, J.-C. Achard, F. Tasset, Rare Earth in Modern Science and Technology, Rare Earths Research Conference, 2 (1980) 585–591.
- [9] V. Favre-Nicolin, R. Cerny, J. Appl. Cryst. (2002) submitted, see also <http://objcryst.sourceforge.net>
- [10] D.G. Westlake, J. Less-Common Met. 90 (1983) 251.
- [11] E. Teatum, K. Gschneider, J. Waber, (1960), LA-2345, U.S. Department of Commerce, Washington, D.C. (cf. book The Crystal Chemistry and Physics of Metals and Alloys, W.B. Pearson p. 151).